G. F. LEAL FERREIRA and O. N. OLIVEIRA, JR.: Hole Transport in 12 µm FEP Samples

phys. stat. sol. (a) 105, 531 (1988)

# Subject classification: 72.20; S12 Instituto de Fisica e Quimica de São Carlos, Universidade de São Paulo, São Carlos¹) 7 Charged 12 µm Sheldahl JAN 1989 Schubweg Model

 $\mathbf{B}\mathbf{y}$ 

G. F. LEAL FERREIRA and O. N. OLIVEIRA, JR.

Potential build up and decay curves for positive corona-charged 12 µm Sheldahl FEP foils are measured and best interpreted using the conventional field-dependent schubweg and a trap structure as follows: shallow traps at the polymer surface (mean life time of 103 s) and quasi-deep traps (mean detrapping time of  $7 \times 10^3$  s) in the bulk. For this trap, only the product of the mobility by the trapping time is relevant (of the order of 10<sup>-10</sup> cm<sup>2</sup>/V). Comparison between measurements in pure No, dry air, and ambient air demonstrates that moisture has a not negligible effect on the charge transport, decreasing the surface potential. Evidence is obtained that holes trapped at the surface are located a little beneath the polymer surface confirming previous measurement by von Seggern through heat pulse technique.

Aufbau und Abfall des Oberflächenpotentials von in einer Koronaanordnung positiv aufgeladenen 12 µm dicken FEP-Folien (Sheldahl) werden untersucht. Die Resultate können am besten gedeutet werden unter der herkömmlichen Annahme eines feldabhängigen Schubwegs. Es ergibt sich eine Haftstellenverteilung mit flachen Haftstellen (Trägerverweilzeit 10°s) an der Folienoberfläche und mitteltiefe Haftstellen (Trägerverweilzeit  $7 imes 10^3$  s) im Innern. Dabei ist aber nur das Produkt von Beweglichkeit und Einfangzeit von Bedeutung, das einen Wert von der Größenordnung 10<sup>-10</sup> cm<sup>2</sup>/V hat. Ein Vergleich von Messungen in reinem N2, trockener Luft und Laboratoriumsluft zeigt, daß Feuchtigkeit das Oberflächenpotential verkleinert und somit einen nicht unwesentlichen Einfluß hat. Es wird ferner gefunden, daß Löcher leicht unter der Oberfläche der Folien eingefangen werden, in Übereinstimmung mit früheren Messungen von von Seggern, die mit der Wärmeimpulsmethode erhalten werden.

## 1. Introduction

Hole transport measurements in 25 µm Dupont Teflon FEP foils has recently been interpreted [1, 2] using a field-independent schubweg. As the schubweg s is  $\mu E \tau$ , one of the parameters  $\mu$  (mobility) or  $\tau$  (trapping time) should be inversely proportional to the electric field E. The latter hypothesis is justified within the scope of either onedimensional conduction [3, 4] or hopping transport for large happing distances at not too high fields [5]. Such a model was suggested by the linear behaviour of the surface potential U versus time t plot in the end of the charging process with a constant corona current.

We have started the present work aiming to confirm the constant schubweg assumption for a set of 12 µm Sheldahl Teflon FEP samples corona-charged mostly in ordinary air, but also in  $N_2$  and in dry air. However, from our measurements, also carried out with the constant-current corona triode, it was deduced that the usual field-dependent schubweg [6, 7] model is more appropriate to explain the results than the field-independent one, unless the field is very low, when both models work the same.

In the following we report measurements of voltage build-up and decay in samples charged positively by corona discharge and the fitting procedure in which the standard

<sup>1)</sup> Caixa Postal 369, São Carlos, Brazil.

600

900

set of partial differential equations have been computer integrated. A simplified model is also presented, which gives a direct insight on the transport mechanism and leads to reasonable results.

The measurements in pure N<sub>2</sub> and in dry air presented here show that the moisture has a non-negligible effect on the charge transport in FEP, as also observed, but in a stronger fashion, in PVDF [8].

The experimental results are presented in Section 3, while Section 2 deals with the experimental procedure. An analysis of the results is given in Section 5 where the theoretical models from Section 4 are developed.

# 2. Experimental

We have used in the present work the corona triode with constant current previously described in other papers [8 to 10]. This apparatus allows the measurement of the sample surface potential during the corona charging as well as after the corona is switched off.

The samples were one-sided metallized Sheldahl Teflon FEP 12  $\mu m$  thick foils, the central electrode having 3.6 cm diameter, surrounded by a guard ring of 6.5 cm external diameter. An air ring of 1.0 mm diameter isolated the measuring electrode from the guard ring. The samples were positively charged with a constant current in air and also, in some experiments, in  $N_2$  and in dry air. Unless otherwise stated, the measurements were made in humid air (50% relative humidity). The currents used were in the range from 0.25 to 1.5 nA.

# 3. Results

Fig. 1 shows typical surface potential build-up and decay curves for a positively charged sample with a current  $I_0 = 0.5$  nA. The solid curves are experimental ones. In the

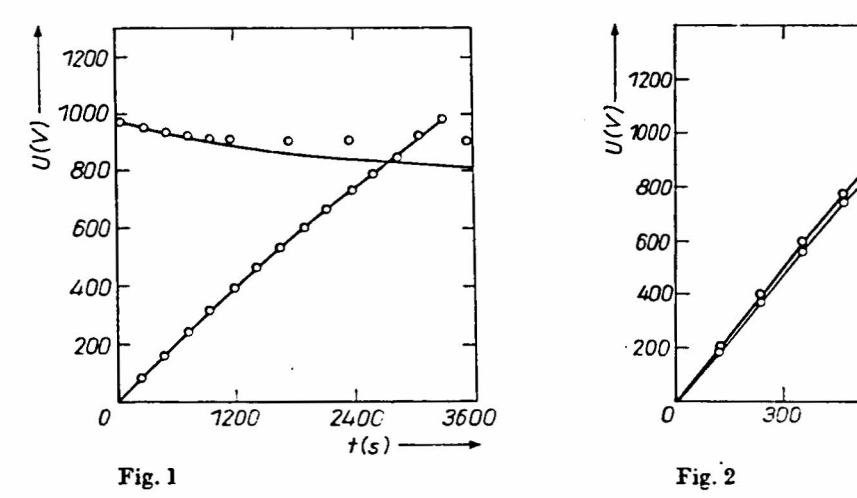


Fig. 1. Potential curves for charging and decay of a  $12 \,\mu m$  FEP sample (number 4 in Table 1) submitted to a current  $I_0 = 0.5$  nA in ambient air. The circles represent theoretical points obtained from the model of Section 4.1 (relative humidity 50%)

Fig. 2. U vs. t plots for the (1) first and (2) second potential build-up of a 12  $\mu$ m FEP sample with a current  $I_0 = 2.0$  nA in ambient air. The circles represent theoretical points calculated using the model of Section 4.1 (relative humidity 50%)

beginning of the charging, the potential increases linearly with time, denoting a capacitive behaviour. The bending observed afterwards indicates that carriers are now being injected into the bulk. The time derivative of the potential, dU/dt, decreases slowly and, at the maximum voltage ( $\approx 1000 \text{ V}$ ), the steady state is far from being reached. The decay curve is shown with a shifted time origin. We take as zero the time when the corona was switched off.

In another set of experiments, the potential after the first run (Fig. 2, curve 1, solid line) was cancelled out using a negative corona current and the sample was then recharged positively (curve 2, solid line). The charging current in both cases was  $I_0 = 2.0$  nA. It is interesting to note the difference in the derivative dU/dt at t = 0. This seems to indicate a decrease of the capacity but, as we shall show later, this is not the case.

A set of samples were corona-charged in pure  $N_2$ . The overall behaviour of the potential curves was the same as those in air, but the surface potential reached higher values than that in air for the same charging time. Furthermore the decay was somewhat slower than in air, but it became faster when ambient air was introduced into the chamber. Measurements carried out in dry air gave results very close to those with nitrogen. The same behaviour had already been observed by the authors in  $25~\mu m$  FEP foils.

## 4. Theory

In [1] results in 25  $\mu$ m Teflon samples were interpreted using basically two hypotheses: 1. surface traps capturing the incoming current and thermally delivering carriers (holes) to the bulk; 2. a constant schubweg for these carriers before bulk trapping. The first hypothesis will be kept in this work, while the second one will be changed to the more conventional hypothesis of a field-dependent schubweg: however, in some calculations we also used the constant schubweg hypothesis for comparison of the results with other ones.

In the following we first present a simplified model, which gives reasonable results. The exact calculation is shown afterwards.

## 4.1 Simplified model

For the surface potential build-up we write

$$\frac{\mathrm{d}U}{\mathrm{d}t} = \frac{i_0 d}{\varepsilon} - \frac{v s \sigma}{\varepsilon},\tag{1}$$

where  $i_0$  is the constant current density, U the surface potential, t the time counted after switching on the corona, d the sample thickness, v the attempt-to-escape frequency,  $\sigma$  the charge density on the sample surface, s the schubweg of the carriers, and  $\varepsilon$  the sample dielectric permittivity (taken as  $1.77 \times 10^{-13}$  F/cm for FEP).

We arrived at the above expression based upon the following intuitive reasoning: assuming negligible free charge accumulation in the sample bulk, the potential increases with the current impinging on the sample surface and decreases due to the injection into the bulk, proportionally to the surface charge and to the schubweg, taken as  $s = \mu \tau U/d$ , where  $\mu$  is the mobility and  $\tau$  the trapping time. The charge kinetics at the sample surface, the same as in [1], is given by

$$\frac{\mathrm{d}\sigma}{\mathrm{d}t} = i_0 - \nu\sigma \,, \tag{2}$$

whose solution is

$$\sigma(t) = \frac{i_0}{v} (1 - e^{-vt}). \tag{2'}$$

Using (2) in (1), we get

$$\frac{\mathrm{d}U}{\mathrm{d}t} = \frac{i_0 d}{\varepsilon} - \frac{\mu \tau i_0 U (1 - \mathrm{e}^{-\tau t})}{\varepsilon d}.$$
 (3)

The formal solution of this differential equation is

$$U(t) = \frac{i_0 d}{\varepsilon} \exp \left\{ -\frac{\mu \tau i_0}{\varepsilon d} \left[ t + \frac{1}{\nu} \left( e^{-\nu t} - 1 \right) \right] \right\} \int_0^t \exp \left\{ \frac{i_0 \mu \tau}{\varepsilon d} \left[ t' + \frac{1}{\nu} \left( e^{-\nu t'} - 1 \right) \right] \right\} dt'. (4)$$

Fitting of the experimental results will provide the values of  $\mu\tau$  and  $\nu$ .

Following the same reasoning, it is easy to get for the surface potential after the corona is switched off

$$U(t) = U_{\rm f} \exp \left\{ -\frac{\mu \tau i_0}{\nu d\varepsilon} \left[ 1 - e^{-\nu(t-t_0)} \right] \right\} \quad \text{for} \quad t > t_0 , \qquad (5)$$

where  $t_d$  is the instant when the corona is switched off and  $U_f$  the potential at  $t_d$ .

#### 4.2 The detailed model

The dynamics of the charges on the surface follows (2). The basic equations for the charge transport in the absence of ohmic conduction and diffusion are

$$\varepsilon \frac{\partial E}{\partial x} = \varrho_{\rm f} + \varrho_{\rm c} \,, \tag{6}$$

Poisson equation, where  $\varrho_t$  is the free charge in the bulk,  $\varrho_t$  trapped charge in the bulk, x the distance along the thickness counted from the charged sample surface, and

$$i_0 = \mu \varrho_I E + \varepsilon \frac{\partial E}{\partial t}. \tag{7}$$

The rate equation for the charges in traps can be written as

$$\frac{\partial \varrho_{t}}{\partial t} = \frac{\varrho_{f}}{\tau} - \frac{\varrho_{t}}{\tau_{D}},\tag{8}$$

where  $\tau_{\rm D}$  is the detrapping time.

Here we have considered detrapping from bulk traps, a process disregarded in the simplified model, but important to explain the long-range potential decay during discharge (see Fig. 1). These equations were numerically solved through the finite difference method [1] with the following initial and boundary conditions:

$$E(x, 0) = 0$$
,  
 $\varrho_{\rm f}(x, 0) = 0$ ,  
 $\varrho_{\rm t}(x, 0) = 0$ ,  
 $E(0, t) = \sigma(t)/\varepsilon$ ,

where  $\sigma(t)$  is given by (2)

In principle, the fitting will provide the values of the four parameters ( $\mu$ ,  $\tau$ ,  $\tau$ <sub>D</sub>, and  $\tau$ ); however, we have found the fitting to depend only on the product of  $\mu$  and  $\tau$  — as in the simplified model of Section 4.1 — for a large range of variation of both parameters individually. Therefore, the model has three parameters, one more than the simplified model ( $\tau$ <sub>D</sub>).

# 5. Analysis of the Experimental Results

# 5.1 The simplified model

Points in Fig. 1 and 2 indicate the result obtained with the simplified model of Section 4.1, coming out of the integration of (3) by the fourth-order Runge-Kutta method. Table 1, part a, gives the set of the parameter values for nine samples.

Table 1 a) Values of the parameters  $\mu\tau$  and r obtained from the fitting of the potential curves for several samples charged with different constant currents  $I_0$ , using the simplified model of Section 4.1. b) Values of  $\mu\tau$ , r, and  $\tau_D$  using the exact model of Section 4.2 for some of the samples

sample	I <sub>0</sub> (nA)	a)		<b>b</b> )		
		$\mu\tau$ (10 <sup>-10</sup> cm <sup>2</sup> /V)	10-3 s-1)	$\mu\tau$ (10 <sup>-10</sup> cm <sup>2</sup> /V)	(10 <sup>-3</sup> s <sup>-1</sup> )	τ <sub>D</sub> (s)
1	1.0	7.5	2.3	7.9	2.3	5850
2	0.5	4.3	1.6	4.5	1.3	8000
3	1.0	4.6	1.7	5.4	2.3	7500
4	0.5	7.0	0.8			
5	0.25	5.0	1.6			
6	0.75	1.8	1.0			
7	1.5	1.0	0.1			
8	0.5	3.0	1.0			
9	1.0 and 0.75	7.2	0.28			

The considerable dispersion in the values of the parameters  $\mu\tau$  and r does not seem to show a systematic trend and might be attributed to the inhomogeneity of the sample batches. To check this, the current in sample 9 was changed during the charging process. Despite this, a single set of parameters succeeded in fitting both portions of the potential curve.

The same set of parameters found for the charging was used to fit the decay curves. The fitting remains good up to a time of the order of  $\tau_D$ . Thereafter, the neglect of the detrapping process makes the fitting poorer (see the decay curve of Fig. 1).

#### 5.2 Results with the numerical integration of the exact model

As already anticipated, only three parameters,  $\mu\tau$ , r, and  $\tau_D$ , come out of the calculation. A very good fitting is now achieved, including the long-range decay, correcting the misfit observed with the simplified model. This is shown in Fig. 3.

The product  $\mu\tau$  is the most sensitive parameter; its value closely determines the behaviour of the curve in all time scales (this is not the case with the other two parameters  $\nu$  and  $\tau_{\rm D}$ , which are important, at the beginning and at the end of the time

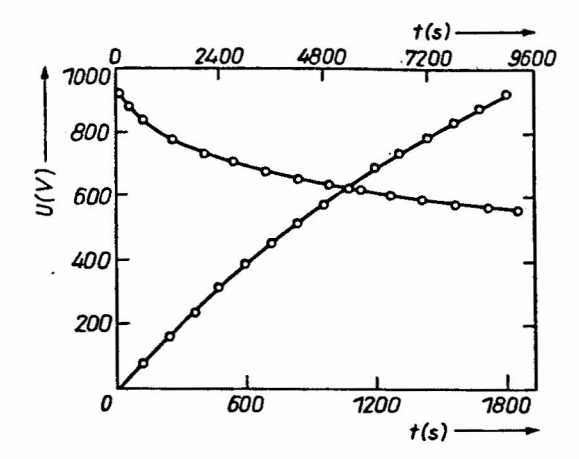


Fig. 3. The same as in Fig. 1, but with a current  $I_0 = 1.0$  nA (sample number 1 in Table 1) and the theoretical points (circles) obtained from the model of Section 4.2. Two different time scales are used, the scale at the bottom for the build-up and the one at the top for the time of decay (relative humidity 50%)

scale, respectively). We have found that the insensitivity of the results to the individual values of  $\mu$  and  $\tau$  prevails for trapping times smaller than 100 s (that is, mobilities not less than  $5 \times 10^{-12}$  cm<sup>2</sup>/Vs). For the accepted value of the mobility as  $2 \times 10^{-9}$  cm<sup>2</sup>/Vs, the trapping time is  $10^{-1}$  s.

The values figuring out in Table 1, part b are not unique in the sense that a 10% change in the product  $\mu\tau$ , accompanied by convenient changes of the other parameters, would also provide a good fitting. The most insensitive parameter is r which may be changed as much as 50% in these adjustments. Note, however, that the changes are not independent and so they are not qualified as errors.

We have also attempted to fit the experimental results with the constant schubweg model as suggested by [1] (the trapping time inversely proportional to the x-dependent electric field). However, we have obtained a good fitting only for those measurements which, according to the previous calculations, had a small schubweg (at most 3 μm) at the end of the charging process. In this case, the fitting was done using a constant schubweg of almost half of the maximum schubweg as given by the other model and slightly lowering the surface attempt-to-escape frequency. In addition we have considered the hopping transport model suggested by von Berlepsch [5]. Here the mobility is field dependent (proportional to  $\sinh(cE)/E$ , with c being a constant) and the drift velocity becomes larger than the thermal velocity, owing to the large hopping distance. Consequently the inverse of the trapping time is proportional to  $\sinh(cE)$ . Since the important quantity for the results is the product  $\mu\tau$  (here inversely proportional to the field) this model leads to analogous results as the previous one (without field dependence of the mobility) and, therefore, of poorer quality than the field-dependent schubweg of Section 4.2. Finally, comparison of parts a and b of Table 1 indicates that the simplified model (and this justifies its presentation here) gives reasonable results indeed.

## 5.3 Comparison with previous results

Multiplying the mean value of  $\mu\tau$  from Table 1 part b, by the electric field corresponding to 1000 V, a schubweg of 4.0  $\mu$ m results. This value is still within the range of the near surface traps detected by von Seggern [12] in 25  $\mu$ m samples and classified as shallow traps, with activation energies up to 1.25 eV. Beside this, von Seggern found a set of bulk traps 1.5 eV deep.

Laborte [13] explains his results on electron beam irradiated 25  $\mu$ m Teflon samples assuming saturable deep traps (10<sup>15</sup>/cm<sup>3</sup>), the mobility as  $2.5 \times 10^{-9}$  cm<sup>2</sup>/Vs, and a trapping time of  $\approx 5$  s, giving  $\mu\tau = 10^{-8}$  cm<sup>2</sup>/V, significantly larger than our values.

If it is true that our Sheldahl 12  $\mu$ m samples behave like the samples used in [12] and [13] (see, however, Section 4), we would say that the trapping characteristics of Table 1 compare better with the near surface traps of von Seggern. Labonte's system is surely related to the bulk and, therefore, with no bearing for our results.

In the next sub-section, some evidence will be brought that the "surface" positive charges reside a little inside the sample. This means that the schubweg, counted from the geometrical surface, would be a little higher than 4.0 µm as mentioned previously.

## 5.4 Second charging results

We return now to the question raised by the result shown in Fig. 2, concerning the change in the initial derivative dV/dt(t=0) when the sample was recharged after neutralizing the positive potential achieved in the first run by a negative corona current. As was pointed out in Section 3 we might think the sample capacity had decreased after the first charging. In order to check this we took a bi-metallized virgin sample and measured the capacity using a capacitance bridge General Radio Type 716C. Then, one of the electrodes was extracted out and the sample submitted to a positive corona discharge. Next, the uncoated face was metallized and the capacity measured again. No difference was detected. Although not shown in Fig. 2, the decrease of the potential during the cancellation process was also measured and it was possible to establish that the linear rate of potential decrease led to the same capacity value as that observed under recharging. The conclusion drawn from these facts is that the positive "surface" charge is located beneath the geometrical surface by about 0.5 µm in these nominally 12 µm samples. The curves in Fig. 2 were fitted using the model of Section 4.1 with the sample thickness 5% smaller in the first run than in the second one and assuming that negative charge, during cancellation, sticks at the geometrical surface and positive charge during recharging recombines with the negative charge accumulated in that way. Our results confirm previous findings by Moreno and Gross [14].

## 5.5 Results in N2 and in dry air

As mentioned at the end of Section 3, measurements in  $N_2$  and in dry air afforded essentially identical results, giving slightly higher potentials as compared with those in ambient air. The following seems to be a consequence of this observed behaviour: a) the ionic carrier in the gas corona does not matter at all for the process going on inside the sample, this implying that holes are involved in the transport process, as usually accepted; b) absorbed water is the species responsible for the lower potentials in ambient air. This conclusion was reinforced by the result in which the decay became faster when the air was substituted for  $N_2$  after a charging procedure in  $N_2$  (figure not shown here).

Analysis of the potential curves in  $N_2$  corona charged samples showed a corresponding decrease of the parameter  $\mu\tau$ , as compared with the value in ambient air. On the other hand, the considerable insensitivity of the potential to the attempt-to-escape surface frequency prevented the study of the moisture relevance to this process.

Finally, we have assumed that all the impinging charges from the corona source are trapped on the surface before being thermally released. This interpretation is consistent with the conduction current conservation relation (CCCR) [15] observed to

hold in the measurements reported here (the CCCR implies a relation between the time derivatives of the potential before and after the corona current is discontinued and the initial time derivative). However, we have carried out some measurements with higher electric field (above 1 MV/cm), not presented here, where CCCR is observed not to hold, indicating direct injection of short-lived carriers into the bulk [15]. We have not attempted a model including this effect.

We have throughly assumed the transport to be due to holes, as the large difference between the behaviour of positively and negatively charged samples seems to indicate. Results with negatively charged 12 µm Sheldahl samples are reported in [16].

## 6. Conclusions

The analysis carried out here seems to show that a field-dependent schubweg prevails in the Scheldahl samples studied here. This conflicts with conclusions derived in previous work in Dupont Teflon FEP for which a constant schubweg held. Of course, the difference may be ascribed to differences in sample processing between manufacturers, but it seems that even the thickness bears some relevance at least for negative transport (in [17] free electrons formed by irradiation are immobile in 25  $\mu$ m Teflon samples, while "corona" electrons are mobile in 12  $\mu$ m [16, 18] both in Dupont samples). If such a "thickness" effect holds for hole transport, is not yet clear. Even aging seems to change the sample behaviour: a sample taken from the same batch used two years ago and leading to the results reported in [1], gave now a response nearer to the result shown in this article.<sup>2</sup>) Therefore, more study is necessary in order to clarify these points.

From our results, the value of  $\mu\tau$  is especially interesting, of the order of  $10^{-10}$  cm<sup>2</sup>/V: it is very close to the one found for negative charge in recent works [16, 18].

Finally it should be stressed that a field-dependent mobility as suggested in [5], but with a constant trapping time, cannot be ruled out. This is left to a later work.

## Acknowledgements

The authors wish to thank very much to Dr. J. A. Giacometti for his collaboration in the experiments and his helpful discussions, to the collegue Mariangela T. Figueiredo for preparing the computer programs used, and to Prof. B. Gross for his interest and discussions of the results. They express their gratitude to the FAPESP for the grant given to one of them (O.N.O.J.). The use of computing resources from DFCM, partially supported by CNPq, is also acknowledged.

## References

- [1] B. Gross, J. A. GIACOMETTI, and G. F. LEAL FERREIRA, Appl. Phys. A 37, 89 (1985).
- [2] H. von Seggern, B. Gross, and D. A. Berkley, Appl. Phys. A 34, 163 (1984).
- [3] E. B. Wilson, J. Phys. C 13, 2885 (1980).
- [4] J. SWORAKOWSKI and G. F. LEAL FERREIRA, J. Phys. D 17, 135 (1984).
- [5] H. von Berlepsch, phys. stat. sol. (a) 90, K97 (1985).
- [6] A. Rose. Phys. Rev. 97, 322; 1538 (1955).
- [7] J. F. FOWLER, Proc. Rov. Soc. A236, 464 (1956).
- [8] B. GROSS, J. A. GIACOMETTI, G. F. LEAL FERREIRA, O. N. OLIVEIRA, JR., J. appl. Phys. 56, 1487 (1984).
- [9] B. Gross, J. A. GIACOMETTI, and G. F. LEAL FERREIRA, Conf. on Electrical Insulation and Dielectric Phenomena, Annu. Rep., IEEE Piscataway (N.J.) 1981 (p. 39).

<sup>2)</sup> We acknowledge Dr. J. A. Giacometti for this information.

- [10] B. GROSS, J. A. GIACOMETTI, and G. F. LEAL FERREIRA, IEEE Trans. Nuclear Sci., 28, 4513 (1981).
- [11] G. E. FORSYTHE and W. R. WASOW, Finite Difference Methods for Partial Differential Equations, John Wiley, New York 1967 (pp. 15 to 37).
- [12] H. von Seggern, J. appl. Phys. 52, 4081 (1981).
- [13] K. LABONTE, IEEE Trans. Nuclear Sci. 29, 1650 (1982).
- [14] R. A. Morena and B. Gross, J. appl. Phys. 47, 3397 (1976).
- [15] G. F. Leal Ferreira, L. N. Oliveira, O. N. Oliveira, Jr., and J. A. Giacometti, Proc. Internat. Symp. on Electrets, ISE5, IEEE Electrical Insulation, Eds. G. M. Sessler and R. G. Multhaupt, Heidelberg 1985 (p. 53).
  IEEE Trans. Electrical Insulation 21, 275 (1986).
- [16] O. N. OLIVEIRA, JR. and G. F. LEAL FERREIRA, App. Phys. A 42, 213 (1987).
- [17] B. GROSS, G. M. SESSLER, and J. E. WEST, J. Appl. Phys. 45, 2841 (1974).
- [18] J. A. GIACOMETTI, G. F. LEAL FERREIRA, and B. GROSS, phys. stat. sol. (a) 88, 297 (1985).

(Received August 17, 1987)

Campo	Dado		
****	Documento 1 de 1		
No. Registro	000776664		
Tipo de material	ARTIGO DE PERIODICO - NACIONAL		
Entrada Principal	Leal Ferreira, Guilherme Fontes		
Título	Hole transport in corona-charged 12 'MU'm sheldahl fep samples interpreted through a field-dependent schubweg model.		
Imprenta	Berlin, 1988.		
Descrição	p.531-9.		
Autor Secundário	Oliveira Júnior, Osvaldo Novais de		
Fonte	Physica Status Solidi (A), Berlin, v.105, n.2, p.531-9, fev. 1988		
Unidade USP	IFQSC-F INST DE FÍSICA DE SÃO CARLOS		
Unidade USP	IFQSC-F INST DE FÍSICA DE SÃO CARLOS		
Localização	IFSC PROD000735		